

Compact Pillbox Reflector Based on Geodesic Lens

D. Pérez-Quintana^{1,2}, Q. Chen³, M. Beruete^{1,2}, O. Quevedo-Teruel³

¹ Public University of Navarra, Department of Electrical, Electronic and Communication Engineering, Spain

² Institute of Smart Cities (ISC), Public University of Navarra, Navarra, Spain

³ Royal Institute of Technology, Stockholm, Sweden
dayanpq@kth.se

Abstract – We propose a pillbox antenna in combination with a geodesic lens at 60 GHz. The antenna is implemented in a dual-layer parallel plate waveguide. The waves from a geodesic lens in a first layer, after being reflected by a parabolic mirror connecting the rims of the two layers, enter a second layer and illuminate the radiation aperture. Since the lens produces a virtual focus, the reflector works as if it is fed from that focus, making the system more compact.

I. INTRODUCTION

The increasing operational frequency in modern wireless communications and radar systems requires cost-effective antennas with beam scanning capabilities. Planar quasi-optical beamformers, such as Luneburg lenses [1], Rotman lenses [2] and pillbox antennas [3], are being considered for these applications. Among all quasi-optical beamformers, geodesic lenses stand out due to their wide scanning range and high efficiency [4]–[7]. Such a lens is usually fed by multiple feedings placed at its periphery, and its rotational symmetry ensures a scanning angle up to $\pm 60^\circ$ with negligible scan losses. These lenses have low losses since they are implemented in a curved parallel plate waveguide that emulates a gradient-index profile. The lens profile is usually obtained by solving a canonical Luneburg inverse problem with a pair of pre-specified foci that must be real. However, this concept can be extended to produce a virtual focus on the same side as the source point of the lens by solving a complementary Luneburg inverse problem [8].

In this work, a complementary Luneburg lens with a virtual focus is employed to illuminate a planar reflector for achieving a compact footprint. The antenna is realized with a dual-layer parallel plate, namely a pillbox structure [9-11]. The design procedures follow two steps. First, the feeding contour for the reflector is found using a ray-tracing analysis that evaluates the directivity, side lobe levels (SLLs), and scanning range. Then the lens is designed so it is fit to this feeding profile. Finally, a full-wave simulation of the whole system is carried out for a final verification.

II. ANALYSIS RESULTS

The ray-tracing configuration of the parabolic reflector is illustrated in Fig. 1(a) with the origin of coordinates placed at the vertex of the parabola. The rays emitted from a horn feed (p_s) reach the parabolic reflector of diameter D and focal distance F , with $F/D = 0.75$. To avoid the blockage effects, a dual-layer (pillbox) reflector is assumed. The beam scanning is realized by moving the feeding source off the focus. In consequence, it produces a beam deviation factor (BDF) in the radiation pattern [12]. Therefore, it is crucial to find the best positions of the source that minimize the BDF. The source can be placed within the boundaries of the gray box shown in Fig. 1(a) defined by $\pm D/2$ ($D = 110$ mm) and $p_s \pm y_{\text{mov}}$ (where $y_{\text{mov}} = 10$ mm is the maximum horizontal displacement from the focal

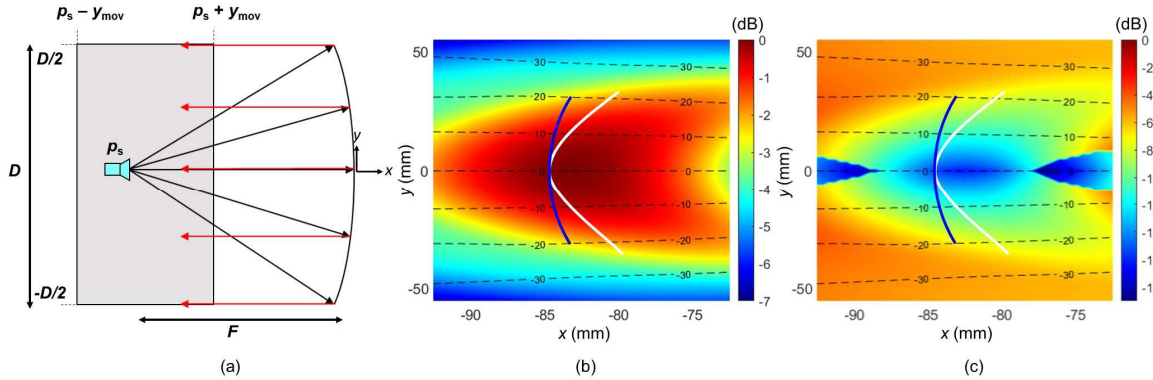


Fig. 1. (a) Schematic of the analyzed problem with a horn feed illuminating a parabolic reflector. The black rays represent those in the first layer and the red ones those in the second layer. (b) Contour plot of the normalized radiation pattern (in dB) as a function of the position of the feed along x and y (the analysis is restricted to the gray area (a)). (c) SLL in dB with respect to the maximum. The dashed lines in (b) and (c) represent the angle of the main beam after reflection by the parabolic mirror. The white curves in (b) and (c) approximate the optimal positions.

point, $p_s = -82.5$ mm). The study of the optimal source location was done using an in-house ray-tracing program with which we obtain the radiation pattern.

Fig 1(b) shows a contour plot of the normalized (to the maximum of the broadside beam) radiation pattern as a function of the source position, varied along x and y in steps of 0.5 mm within the gray area. The maximum directivity values appear near the focus. However, if the feeding source is moved away from the focus, the directivity decreases due to the BDF. The dashed lines in the plot indicate the main beam angle. Likewise, Fig. 1(c) shows the SLL in dB. The behavior is similar to the directivity results: close to the focus the SLL is below -10 dB and increases when the source is displaced from that point. Analyzing the graphs, it is found that to achieve the greatest possible scanning angle while maintaining a high directivity and low SLL, the feeding source should move along the white curve shown in Figs. 1(b) and (c).

In the next step, we study the behavior of a dual-layer system composed by a geodesic lens (radius equal to 5λ , with λ the wavelength at 60 GHz, centered at the operational band) with a virtual focus at 7λ from the lens center and a parabolic reflector placed at 9λ from the center to the geodesic lens with $F/D = 0.75$ and $D = 110$ mm, see sketch in Fig. 2(a). The Transient Solver of commercial simulator CST Microwave Studio® was used to simulate the system. As shown in Fig. 2(a), the profile height of the geodesic lens is reduced by applying a two-folding operation [4]. Eleven WR-15 waveguide ports were placed along the periphery to feed the geodesic lens.

With the previous study, we have found that the optimal location of a point source follows the white curve in the insets of Fig. 1(b) and (c). However, due to the rotational symmetry of a Luneburg geodesic lens, the feeding contour must follow a circular arc, as shown in the blue curve of Fig. 1(b) and (c). This arc has a radius equal to F (the focal length of the parabola), is centered at the origin coordinates with maximum aperture angle $\theta_s = 40^\circ$. Fig. 2(b) shows the normalized radiation pattern obtained for the entire system. The maximum scanning range is around $\pm 18^\circ$. In addition, the directivity decreases by 2.8 dB in the maximum scanning angle close to 18° . These results are in good agreement with the previous analysis of a source moving along the blue arcs in Fig. 1(b), (c). Note that in those figures, the maximum scanning range is near 20° and the directivity at the maximum angle drops by 2.8 dB.

III. CONCLUSION

To sum up, this article demonstrates a combination of a dual-layer Luneburg geodesic lens with a parabolic reflector system to produce a compact antenna. First, the optimal positions of a point source feeding the parabolic reflector have been found by an in-house ray-tracing code. Afterwards, a practical implementation with a geodesic lens has been analyzed considering that the virtual source can only move along an arc of circumference. A thorough numerical study has been performed and it has been found that a compact design can be enhanced while keeping

a good directivity level. The results achieved for the dual-layer geodesic lens with a parabolic reflector opens new opportunities for the design of directive antennas, due to the compact design and the good radiation characteristics.

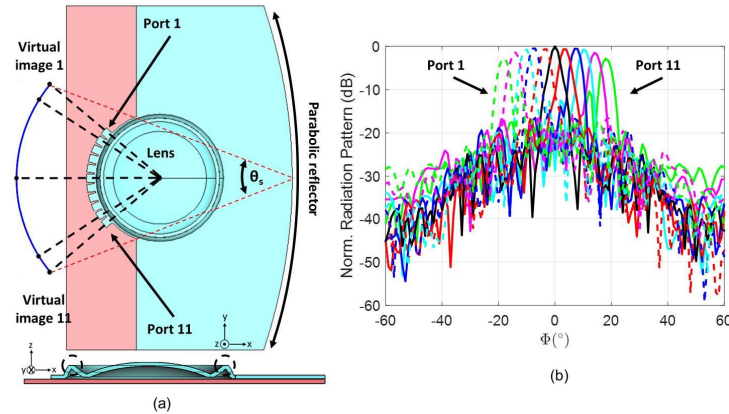


Fig. 2. (a) Schematic of a dual layer geodesic lens integrated with parabolic reflector: (a) Cross-sectional view of both layers, blue layer represents the top layer and the red one the bottom. (b) Normalized radiation pattern of the dual layer geodesic lens integrated with the parabolic reflector.

ACKNOWLEDGEMENT

Project RTI2018-094475-B-I00 funded by MCIN/ AEI /10.13039/501100011033/ FEDER “Una manera de hacer Europa”. This article is based upon work from COST Action SyMat CA18223, supported by COST (European Cooperation in Science and Technology), www.cost.eu.

REFERENCES

- [1] R. K. Luneburg, *Mathematical Theory of Optics*. University of California Press, 1964.
- [2] W. Rotman and R. Turner, “Wide-angle microwave lens for line source applications,” *IEEE Trans. Antennas Propag.*, vol. 11, no. 6, pp. 623–632, Nov. 1963, doi: 10.1109/TAP.1963.1138114.
- [3] E. Shannon, “Wide-Angle Scanning with Microwave Double-Layer Pillboxes,” vol. 2, 1957.
- [4] K. S. Kunz, “Propagation of Microwaves between a Parallel Pair of Doubly Curved Conducting Surfaces,” *J. Appl. Phys.*, vol. 25, no. 5, pp. 642–653, May 1954, doi: 10.1063/1.1721704.
- [5] O. Quevedo-Teruel *et al.*, “Geodesic Lens Antennas for 5G and Beyond,” *IEEE Commun. Mag.*, vol. 60, no. 1, pp. 40–45, Jan. 2022, doi: 10.1109/MCOM.001.2100545.
- [6] Q. Liao, N. J. G. Fonseca, and O. Quevedo-Teruel, “Compact Multibeam Fully Metallic Geodesic Luneburg Lens Antenna Based on Non-Euclidean Transformation Optics,” *IEEE Trans. Antennas Propag.*, vol. 66, no. 12, pp. 7383–7388, Dec. 2018, doi: 10.1109/TAP.2018.2872766.
- [7] N. J. G. Fonseca, Q. Liao, and O. Quevedo-Teruel, “Equivalent Planar Lens Ray-Tracing Model to Design Modulated Geodesic Lenses Using Non-Euclidean Transformation Optics,” *IEEE Trans. Antennas Propag.*, vol. 68, no. 5, pp. 3410–3422, 2020, doi: 10.1109/TAP.2020.2963948.
- [8] N. J. G. Fonseca, T. Tyc, and O. Quevedo-Teruel, “A solution to the complement of the generalized Luneburg lens problem,” *Commun. Phys.*, vol. 4, no. 1, p. 270, Dec. 2021, doi: 10.1038/s42005-021-00774-2.
- [9] W. Rotman, “Wide-angle scanning with microwave double-layer pillboxes,” *IRE Trans. Antennas Propag.*, vol. 6, no. 1, pp. 96–105, Jan. 1958, doi: 10.1109/TAP.1958.1144548.
- [10] M. Ettore, R. Sauleau and L. Le Coq, “Multi-Beam Multi-Layer Leaky-Wave SIW Pillbox Antenna for Millimeter-Wave Applications,” *IEEE Trans. Antennas Propag.*, vol. 59, no. 4, pp. 1093–1100, April 2011, doi: 10.1109/TAP.2011.2109695.
- [11] T. Ströber, S. Tubau, E. Girard, H. Legay, G. Goussetis and M. Ettore, “Shaped Parallel-Plate Lens for Mechanical Wide-Angle Beam Steering,” *IEEE Trans. Antennas Propag.*, vol. 69, no. 12, pp. 8158–8169, Dec. 2021, doi: 10.1109/TAP.2021.3090789.
- [12] Y. Lo, “On the beam deviation factor of a parabolic reflector,” *IRE Trans. Antennas Propag.*, vol. 8, no. 3, pp. 347–349, May 1960, doi: 10.1109/TAP.1960.1144854.